[2] J. J. Lee and C. S. Park, "60-GHz gigabits-per-second OOK modulator with high output power in 90-nm CMOS," *IEEE Trans. Circuits Syst. II, Express Briefs*, vol. 58, no. 5, pp. 249–253, May 2011.
[3] K.-S. Chin, W. Jiang, W. Che, C.-C. Chang, and H. Jin, "Wideband LTCC 60-GHz antenna array with a dual-resonant slot and patch structure," *IEEE Trans. Antennas Propag.*, vol. 62, no. 1, pp. 174–182, Jan. 2014.
[4] Z. Briqech, A. R. Sebak, and T. A. Denidni, "High-efficiency 60-GHz printed yagi antenna array," *IEEE Antennas Wireless Propag. Lett.*, vol. 12, pp. 1224–1227, 2013.
[5] L. Wang, Y.-X. Guo, and W.-X. Sheng, "Wideband high-gain 60-GHz LTCC L-probe patch antenna array with a soft surface," *IEEE Trans. Antennas Propag.*, vol. 61, no. 4, pp. 1802–1809, Apr. 2013.
[6] H. Chu, Y.-X. Guo, and Z. Wang, "60-GHz LTCC wideband vertical off-center dipole antenna and arrays," *IEEE Trans. Antennas Propag.*, vol. 61, no. 1, pp. 153–161, Jan. 2013.
[7] Y. Li and K.-M. Luk, "A 60-GHz dense dielectric patch antenna array," *IEEE Trans. Antennas Propag.*, vol. 62, no. 2, pp. 960–963, Feb. 2014.
[8] B. Zhang and Y. P. Zhang, "Grid array antennas with subarrays and multiple feeds for 60-GHz radios," *IEEE Trans. Antennas Propag.*, vol. 60, no. 5, pp. 2270–2275, May 2012.
[9] F. Yang, X.-X. Zhang, X. Ye, and Y. Rahmat-Samii, "Wide-band E-shaped patch antennas for wireless communications," *IEEE Trans. Antennas Propag.*, vol. 49, no. 7, pp. 1094–1100, Jul. 2001.
[10] T. Jang, H. Y. Kim, I. S. Song, C. J. Lee, and C. S. Park, "Low-profile wideband E-shaped patch antenna for 60 GHz communication," in *Proc. Asia Pacific Microw. Conf. (APMC)*, Nanjing, China, Dec. 2015, pp. 1440–1442.
[11] Y. Wang, "A series feed E-shaped microstrip antenna with high gain," in *Proc. Int. Symp. Antennas Propag.*, Oct. 2012, pp. 175–178.
[12] C. A. Balanis, *Antenna Theory: Analysis and Design*, 3rd ed. New York, NY, USA: Wiley, 2005.

A Novel Supercell-Based Dielectric Grating Dual-Beam Leaky-Wave Antenna for 60-GHz Applications

Zi Long Ma, Kung Bo Ng, Chi Hou Chan, and Li Jun Jiang

***Abstract*— This communication proposes a novel dual-beam dielectric grating antenna based on the supercell (SC) concept. Through the theoretical analysis of the effective phase constants of the SC, it is found that two space harmonic modes ($m = -1$ and $m = -2$) can be simultaneously excited (above the air line) within a certain frequency range. This phenomenon leads to the generation of two radiation beams in the far-field region. At the frequency where the phase constants satisfy $\beta_{-1} = -\beta_{-2}$, the two beams are in symmetric directions with respect to the axis that is perpendicular to the azimuth plane. Different from the conventional periodic structures that the $m = -2$ mode lacks well control, the proposed antenna can manipulate both modes and obtain equal performance for the two radiation beams. In this communication, the symmetric beam case is investigated. The detailed design principle is presented. In addition, the frequency-based beam steering characteristic that the two beams scan in the same clockwise or anticlockwise direction is discussed as well. The proposed antenna operates in 60-GHz band and it can be a good candidate for the WiGig application.**

***Index Terms*— 60-GHz, dielectric grating antenna, dispersion analysis, dual-beam, leaky-wave, supercell (SC).**

I. Introduction

In recent years, the 60-GHz band has attracted much interest, because of its high transmission rate at the level of Gb/s and the fast-growing demand of unlicensed short-range data links [1]–[3]. Antenna, as a key component of the entire communication system, its design in this frequency band always faces challenges. The fabrication cost, antenna performance and integration ability with other components are often the important design considerations [4]. In the past decades, the difficulties inherent in constructing antennas at millimeter-wave frequencies have spurred interest in dielectric antennas [5]. Thanks to their advantages of low-cost, easy integration and good compatibility, many studies have been conducted and reported. In terms of the antenna configuration, the dielectric antennas can be generally categorized into two types, dielectric rod and periodic grating antennas [5]–[11]. The former type often features end-fire radiation. In [5], the characteristics of linearly and curvilinearly tapered cylindrical dielectric rod antennas are analyzed. For the latter type, the periodic gratings-based dielectric antennas employ leaky-wave principle as the main radiation mechanism. They have more flexible radiation directions and offer the advantage of frequency-based beam steering. The detailed theories of these antennas are presented in [6] and [7]. In [8] and [9], the dielectric grating antennas with omnidirectional patterns are presented. Reference [10] discusses the effects of the grating profile and various

Manuscript received July 27, 2016; accepted September 30, 2016. Date of publication October 25, 2016; date of current version December 5, 2016. This work was supported in part by the Research Grants Council of Hong Kong under Grant GRF 17207114 and Grant GRF 17210815, in part by NSFC under Grant 61271158, in part by the HKU Seed Fund under Grant 201309160052, and in part by CityU SKLMW under Grant 93601030.

Z. L. Ma was with The University of Hong Kong, Hong Kong. He is now with the State Key Laboratory of Millimeter Waves, Partner Laboratory, City University of Hong Kong, Hong Kong (e-mail: mazilong@connect.hku.hk).

K. B. Ng and C. H. Chan are with the State Key Laboratory of Millimeter Waves, Partner Laboratory, City University of Hong Kong, Hong Kong (e-mail: eechic@cityu.edu.hk).

L. J. Jiang is with the Department of Electrical and Electronic Engineering, The University of Hong Kong, Hong Kong.

Color versions of one or more of the figures in this communication are available online at http://ieeexplore.ieee.org.

Digital Object Identifier 10.1109/TAP.2016.2621031

0018-926X © 2016 IEEE. Personal use is permitted, but republication/redistribution requires IEEE permission.
See http://www.ieee.org/publications_standards/publications/rights/index.html for more information.

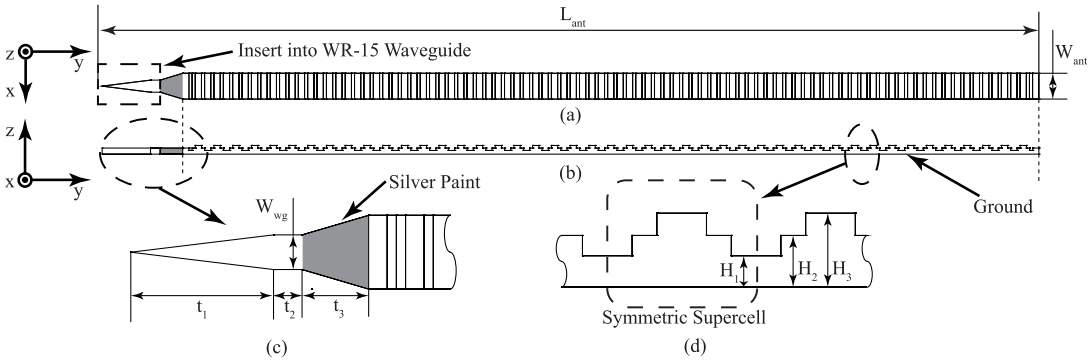

Fig. 1. Configuration of the proposed SC-based dielectric grating dual-beam leaky-wave antenna. (a) Top view. (b) Side view. (c) Waveguide to antenna transition. (d) Proposed symmetric SC.

dimensions on the performance by using the perturbation analysis. A beam electronically switched leaky-wave antenna by using p-i-n diodes is presented in [11].

In modern communication systems, the link quality is often adversely affected by many intrinsic effects, such as multipath effect and mutual interference. One effective solution to minimize these effects is to adopt directional antennas from the physical layer perspective. Dual-beam directional antennas are often desired [12]. In order to excite two radiation beams, various methods can be applied. In [12] and [13], the higher order modes are employed. They use the higher order TM_{02} mode and the second higher order leaky mode, respectively. By using two feeding terminals, dual-beam excitation can be realized as well [14]–[18]. Although in [14] the microstrip patch is fed by a single terminal based on coplanar waveguide, the operation principle is similar to the two-terminal designs. Reference [19] presents a dual-beam microstrip leaky-wave antenna based on a 4×1 phased array. In most of these designs, in order to properly excite the two radiation beams, some extra power dividers and lumped components are employed. These additional circuits may introduce unnecessary power loss and degrade the overall system performance. In addition, the fabrication cost and the system complexity will be increased correspondingly.

In this communication, we propose a novel supercell (SC)-based dual-beam dielectric grating leaky-wave antenna for 60-GHz applications. It not only has the advantages of conventional dielectric antennas, which are low-cost, easy integration and good compatibility, but also features a simple feed. Its operation theory is based on our previous study on dispersion characteristics of multiple periodic structures [20]. In the previous work, we found that the structures that are in the SC (multiple periodic) configuration can easily generate two radiation beams by simultaneously exciting the $m = -1$ and $m = -2$ space harmonic modes. It is well known that the conventional single periodic structures can excite the $m = -2$ space harmonic mode as well [21]. However, they often lack the degree of freedom to properly control this mode. As a result, the beam that dominated by the $m = -2$ mode is often regarded as high side lobes. Substantial efforts have been dedicated in the literature to precisely suppress the excitation of this mode. Different from the conventional structures, the proposed SC-based antenna can manipulate the $m = -2$ space harmonic mode to obtain equal performance for the two beams. At the frequency where the condition $\beta_{-1} = -\beta_{-2}$ is satisfied, the two beams will be symmetric with respect to the axis that is perpendicular to the azimuth plane. Furthermore, in this communication, the frequency-based beam steering property of the proposed antenna is also discussed. With the frequency variation, the two beams can be steered in the same clockwise or anticlockwise direction with small performance variation.

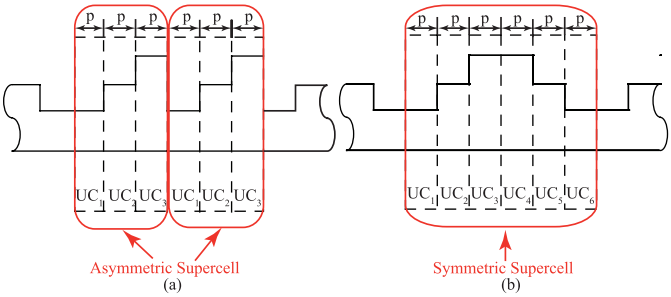

Fig. 2. Illustrations of the configurations of (a) asymmetric and (b) symmetric SCs.

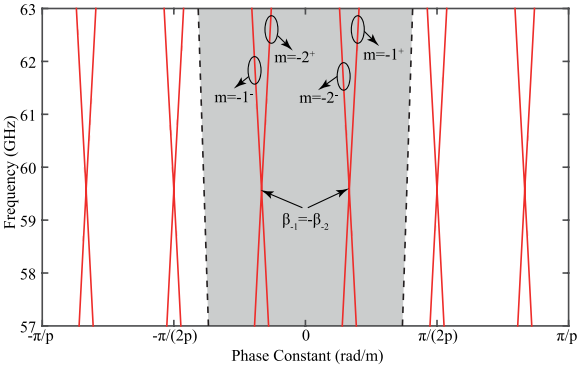

Fig. 3. Phase constants of the proposed symmetric SC. The red curves are the phase constants for various space harmonic modes. The black dashed lines stand for the air lines. The gray region refers to the leaky-wave radiation region.

II. Antenna Configuration

Fig. 1 shows the configuration of the proposed SC-based dielectric grating dual-beam leaky-wave antenna. In Fig. 1(a) and (b), the top and side views of the proposed antenna are presented. The antenna is fed by a standard WR-15 waveguide. The SC-based dielectric grating plays a role in the antenna radiation. On the left side, a transition structure is designed to provide a smooth power transmission from the waveguide to the grating. In Fig. 1(c), the geometrical details of the transition part are presented. The part with length t_1 is linearly tapered and the neighbor part is designed to have the same width W_{wg} with the standard waveguide. In the practical implementation, these two parts are inserted into the waveguide. The third part that is with the length of t_3 is covered by silver paint on the four faces. The height of the entire transition is identical to the feeding waveguide. Fig. 1(d) shows the details of the proposed symmetric SC. It can be observed that the SC is symmetric with respect to the vertical

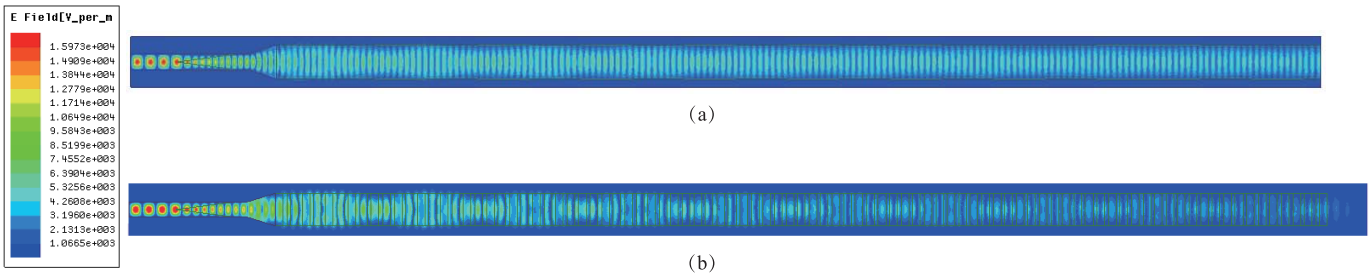

Fig. 4. Full-wave simulated E-filed distributions of (a) grounded dielectric waveguide without corrugations and (b) proposed SC-based dielectric grating dual-beam leaky-wave antenna.

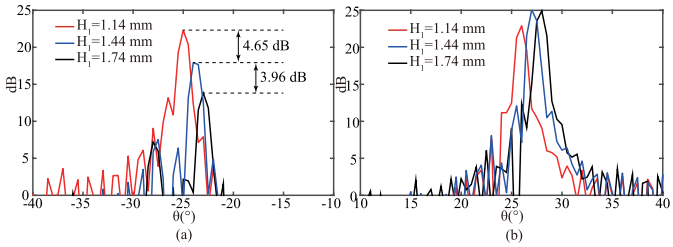

Fig. 5. Simulated copolarized radiation patterns (yz plane) with various H_1 at 60 GHz. (a) Backward beam. (b) Forward beam.

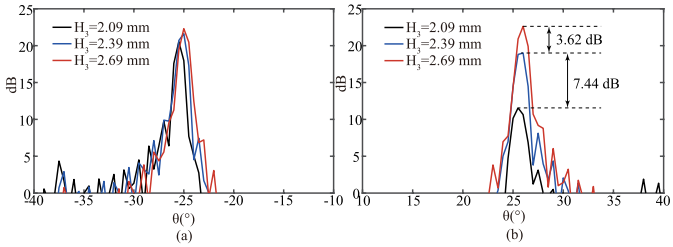

Fig. 6. Simulated copolarized radiation patterns (yz plane) with various H_3 at 60 GHz. (a) Backward beam. (b) Forward beam.

centerline and consists of two height-varying corrugations on each side along the longitudinal direction. Each corrugation can be treated as one unit cell (UC) and all the UCs have the same physical length. The heights from the lowest to the highest are denoted as H_1, H_2, and H_3, respectively. The identical SCs are periodically arranged along one dimension. A prototype of the proposed antenna that contains 45 SCs is demonstrated in this communication. On the backside of the antenna, a ground plane can be found. In this design, the Teflon material is used as the dielectric. Its parameters are $\epsilon_r = 2.1$ and loss tangent $= 0.001$.

III. Theory and Design Principle

In [20], we propose a novel multiple periodic configuration, in which several different series connected UCs form an SC and a number of identical SCs are periodically arranged to compose the antenna. Through the analysis on the effective phase constants of the SC, we have demonstrated that with the same antenna length, the SC-based periodic structures can excite higher order space harmonic modes to radiate at relatively lower frequencies more easily than the conventional counterparts. The more the number of UCs in the SC, the shorter the separation distance (in the phase constant diagram) of the space harmonic modes. Based on this phenomenon, the SC concept is applied to this dual-beam antenna design. In the previous study, it is found that as long as the number of UCs in one SC is larger than one, the $m = -1$ and $m = -2$ modes can be simultaneously excited in a certain frequency range. However, with the increase of the quantity of UCs, the design complexity is increased correspondingly. In view of this consideration, the SC configuration with triple UCs is chosen in this design. The configuration of the initial asymmetric SC is shown in Fig. 2(a). Since the proposed antenna is expected to have symmetric performance, a symmetric SC configuration should be more suitable for this design. Therefore, the SC is finally designed as Fig. 2(b) shows. Comparing the two structures, the symmetric design should be easier to fabricate. The operation principle of the symmetric SC is identical to the previous discussion.

By using the full wave simulation software ANSYS high frequency structural simulator, the effective phase constants of the proposed symmetric SC can be extracted, as shown in Fig. 3. In Fig. 3, the black dashed lines stand for the air lines and the gray region refers to the leaky-wave radiation region. The red curves are the phase constants for various space harmonic modes. They can be expressed by

$$\beta_m(\omega) = \pm\left[\beta_e(\omega) + \frac{2m\pi}{L_{\rm sc}}\right] \quad m = 0, \pm1, \pm2, \pm3 \ldots \tag{1}$$

where m is the mode index, β_e and $L_{\rm sc}$ ($L_{\rm sc} = 6p$) are the effective phase constant and the physical length of the SC. We can observe that, as we expected, from 57 to 63 GHz, two space harmonic modes are above the air lines and with different phase constants. They correspond to $m = -1$ and $m = -2$ modes, respectively. According to the theory of leaky-wave antenna, this phenomenon implies that the structure based on the proposed SC can generate two radiation beams in the far-field region. In addition, at almost 60 GHz, the curves of the two modes are intersected and the phase constants satisfy $\beta_{-1} = -\beta_{-2}$. The well-known relation between the radiation angle (from broadside direction) and the phase constant is defined by

$$\theta \approx \sin^{-1}\left(\frac{\beta_m}{k_0}\right). \tag{2}$$

Therefore, the two resultant beams are symmetric with respect to the xz plane. Furthermore, it is not difficult to find that with the frequency variation, the two beams show in-directional steering. This is different from most existing studies on beam steering dual-beam antenna.

The design of the proposed dual-beam leaky-wave antenna can start from a grounded dielectric waveguide without corrugations. By properly designing the parameters t_1, t_2, t_3, and $W_{\rm ant}$, the grounded dielectric waveguide can be fed from the left side. The E-field distribution inside the dielectric waveguide is presented in Fig. 4(a). It can be seen that after the transition part, the waves are converted from the waveguide mode to the fundamental propagation mode in the dielectric. The E-field shows an almost uniform distribution along the dielectric waveguide. From the left side to the end of the structure, there is no obvious magnitude reduction. It implies that the designed dielectric waveguide can successfully guide the waves.

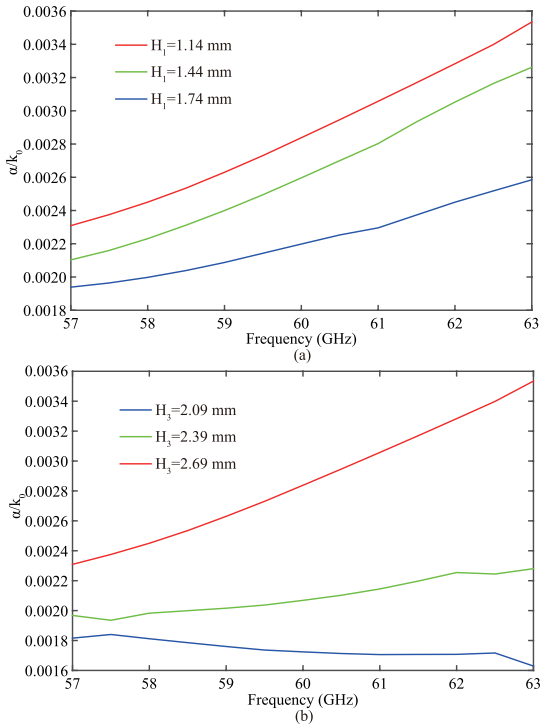

Fig. 7. Normalized attenuation constants for various (a) H_1 and (b) H_3.

After this procedure, the corrugations can be added on the dielectric waveguide. The E-field distribution of the proposed SC-based antenna with optimized parameters is presented in Fig. 4(b). It is seen that the magnitude of the E-field is gradually reduced along the structure due to the leaky-wave radiation.

After adding the corrugations, the radiation performance of the proposed antenna can be investigated. In order to reduce the design complexity, we can keep the parameter H_2 unchanged and gradually adjust H_1 and H_3 to obtained the required gain. Figs. 5 and 6 present the effects of the parameter H_1 and H_3 on the radiation patterns, respectively. In Fig. 5, the patterns stand for the copolarizations in yz plane at 60 GHz. It can be seen that with the increase of H_1, the gain of the backward beam is gradually reduced. In contrast, the gain of the forward beam is less sensitive to this parameter variation. Similarly, in Fig. 6, the gain of the forward beam is increased as H_3 increases while that of the backward beam is almost kept. Therefore, it can be found that the backward and forward beams are almost independently controlled by H_1 and H_3, respectively. According to the aforementioned theory, the two beams correspond to the two space harmonic modes. Therefore, we can conclude that the $m = -2$ and $m = -1$ modes are dominated by H_1 and H_3, respectively. By proper designing these two parameters, the beam pairs with flexible gain can be obtained.

In Fig. 7(a) and (b), the normalized attenuation constants for various H_1 and H_3 are presented, respectively. With the decrease of H_1 and the increase of H_3, the proposed antenna shows a gradually increased attenuation. It implies that more power is radiated by the antenna. All the attenuation constants indicate the total power loss in the structure, namely, the wave attenuation comes from both $m = -1$ and $m = -2$ modes. Since H_1 and H_3 have dominant effects on the $m = -2$ and $m = -1$ modes, approximately, we can think that Fig. 7(a) and (b) stands for the variations of attenuation of the two modes, respectively.

In Fig. 8, effects of various antenna parameters on the phase constants are presented. The effects of the UC length p, overall

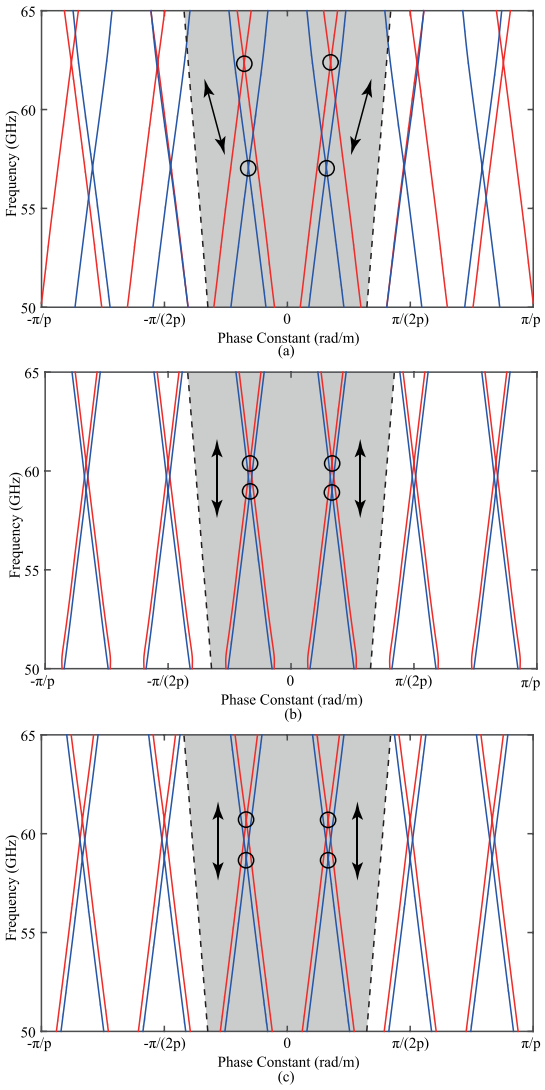

Fig. 8. Effects of various antenna parameters on the phase constants. (a) Various UC length p. The red and blue curves stand for $p = \{0.92, 1.02\}$ mm, respectively. (b) Various overall SC height $(\{H_1, H_2, H_3\} + \delta)$. The red and blue curves stand for $\delta = \{-0.3, 0.3\}$ mm, respectively. (c) Various SC width W_{wg}. The red and blue curves stand for $W_{\mathrm{wg}} = \{4, 20\}$ mm, respectively. The circles indicate the symmetric dual-beam locations.

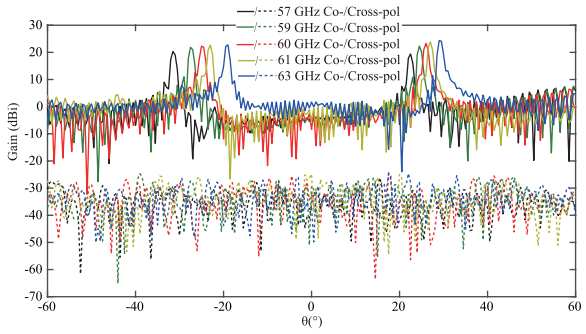

Fig. 9. Simulated radiation patterns in yz plane for the proposed antenna.

SC height $(\{H_1, H_2, H_3\} + \delta)$, and SC width W_{wg} are shown in Fig. 8 (a)–(c), respectively. We can see that for symmetric dual-beam, p provides simultaneous controls in both vertical and horizontal axes, while, δ and W_{wg} adjust the dual-beam points in the vertical axis. These variations imply that the antenna parameters can offer enough

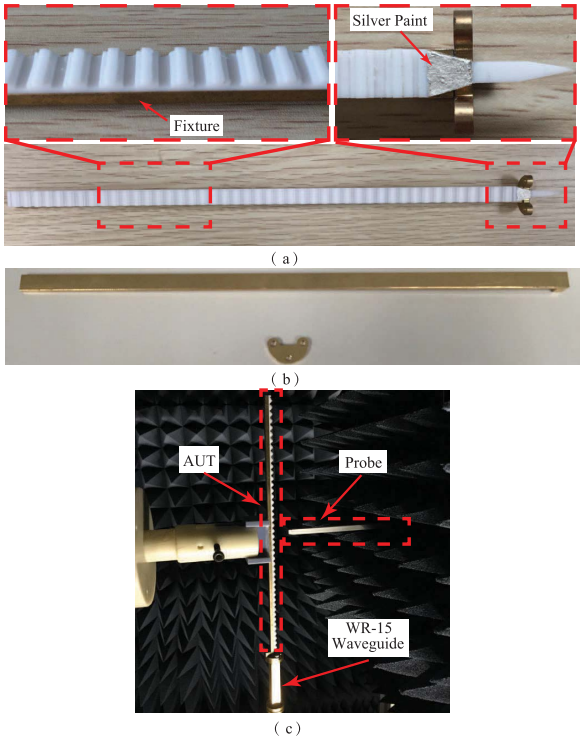

Fig. 10. Photographs of (a) fabricated antenna, (b) fixture, and (c) measurement setup.

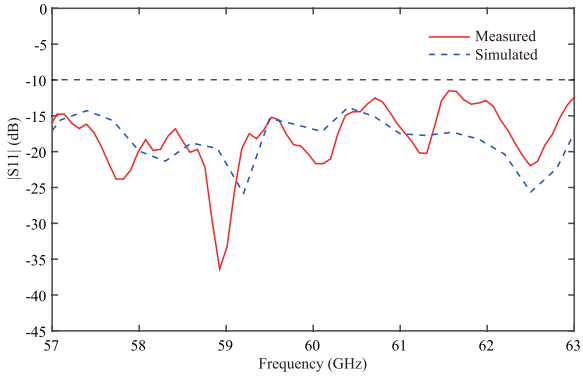

Fig. 11. Measured and simulated magnitudes of S11 for the proposed antenna.

TABLE I
ANTENNA PARAMETERS (mm)

L_{ant}	W_{ant}	W_{wg}	p	H_1	H_2	H_3	t_1	t_2	t_3
290.78	8	3.759	0.97	1.14	1.88	2.69	15	3	7

degree of freedom to manipulate symmetric dual-beam points in the phase constant diagram. Consequently, the operation frequency and beam directions can be adjusted. The optimized antenna parameters are listed in Table I. Fig. 9 shows the full-wave simulated copolarization and cross-polarization patterns in yz plane with optimized geometrical parameters. The frequency range covers the band of the WiGig application. The cross-polarizations within this band are very small.

IV. EXPERIMENTAL RESULTS

In order to verify the proposed idea, the SC-based dielectric grating dual-beam leaky-wave antenna is fabricated and experimentally tested. The photographs of the fabricated antenna and measurement setup are presented in Fig. 10. An extra fixture is designed to not only provide strong support to the soft dielectric but also serve as a ground plane. In the measurement, it is fixed on the flange of the WR-15 waveguide by screws. The antenna is measured in the Nearfield Systems Inc. (NSI) near-field measurement system. The measured and simulated magnitudes of S11 are presented in Fig. 11. It is obvious that the fabricated prototype has very good impedance matching. From 57 to 63 GHz, the measured |S11| is below −10 dB and shows good agreement with the simulation.

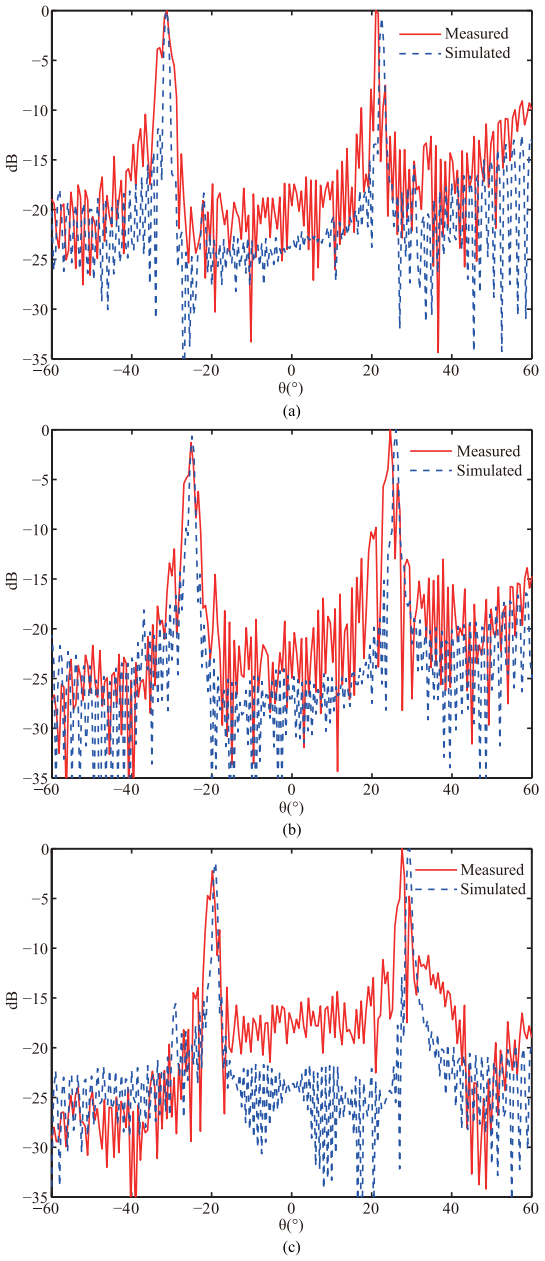

Fig. 12. Normalized measured and simulated radiation patterns (yz plane) at (a) 57, (b) 60, and (c) 63 GHz.

In Fig. 12, the normalized measured and simulated radiation patterns E_θ in yz plane are presented. It can be seen that the measured and simulated patterns show reasonable agreements. Two radiation beams can be clearly observed. At 60 GHz, the proposed antenna is designed to have two symmetric radiation beams. The simulated

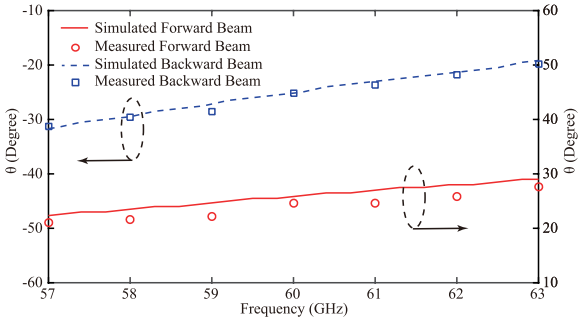

Fig. 13. Measured and simulated angles (from the broadside direction) of the backward and forward beams.

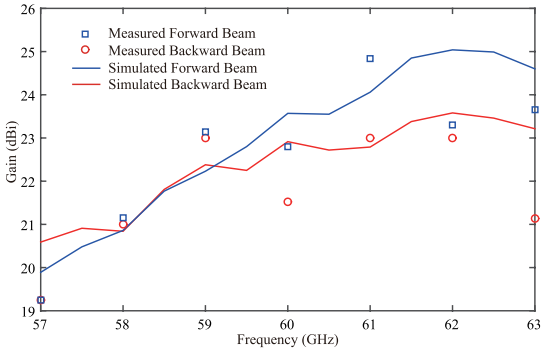

Fig. 14. Measured and simulated gain of the backward and forward beams.

results show that the backward and forward beams are at ±26°, respectively. In the measurement, they appear at −25.2° and 24.6°. The discrepancy is very small. In order to examine the beam steering performance, the normalized measured and simulated patterns at 57 and 63 GHz are presented in Fig. 12(a) and (c), respectively. With the frequency variation, the two beams scan in the same clockwise or anticlockwise direction. Some discrepancies can be found between the measured and simulated results. They may be caused by the unavoidable fabrication tolerance and the difference between the practical implementation and the ideal simulation. In addition, the proposed antenna has narrow beamwidth. In the measurement process, the vibration of the measuring probe (Fig. 10) during movement may also affect the results. The probe is an open-ended waveguide probe which is based on the standard WR-15 waveguide and is provided by NSI. However, from these results, the proposed design idea is validated successfully. Fig. 13 summarizes the measured and simulated angles of the forward and backward beams over the frequency range from 57 to 63 GHz. It can be seen that the measured backward beam directions are almost the same as simulations. The maximum variation is smaller than 1.5°. The measured forward beam angles follow the same trend with the simulation. The variation is about 2°. In Fig. 14, the measured and simulated gain of the backward and forward beams are presented, respectively. The agreements are reasonable. At 60 GHz, the proposed antenna has high gain of 21.5 and 22.8 dBi for the backward and forward beams, respectively.

V. Conclusion

In this communication, an SC-based dielectric grating dual-beam leaky-wave antenna has been proposed, designed, fabricated and tested. The mechanism is analyzed through the dispersion analysis. Two space harmonic modes $m = -1$ and $m = -2$ are excited to generate the dual-beam. At 60 GHz, the proposed antenna has symmetric beams and the two beams have similar properties. The proposed antenna is validated by both full-wave simulation and practical experiment. The results show reasonable agreements. The proposed antenna can be a good candidate for the WiGig application.

References

[1] A. L. Amadjikpe, D. Choudhury, G. E. Ponchak, and J. Papapolymerou, "Location specific coverage with wireless platform integrated 60-GHz antenna systems," *IEEE Trans. Antennas Propag.*, vol. 59, no. 7, pp. 2661–2671, Jul. 2011.

[2] Y. P. Zhang and D. Liu, "Antenna-on-chip and antenna-in-package solutions to highly integrated millimeter-wave devices for wireless communications," *IEEE Trans. Antennas Propag.*, vol. 57, no. 10, pp. 2830–2841, Oct. 2009.

[3] D. Wang, K. B. Ng, C. H. Chan, and H. Wong, "A novel wideband differentially-fed higher-order mode millimeter-wave patch antenna," *IEEE Trans. Antennas Propag.*, vol. 63, no. 2, pp. 466–473, Feb. 2015.

[4] Y. Zhang, Z. N. Chen, X. Qing, and W. Hong, "Wideband millimeter-wave substrate integrated waveguide slotted narrow-wall fed cavity antennas," *IEEE Trans. Antennas Propag.*, vol. 59, no. 5, pp. 1488–1496, May 2011.

[5] T. Ando, I. Ohba, S. Numata, J. Yamauchi, and H. Nakano, "Linearly and curvilinearly tapered cylindrical-dielectric-rod antennas," *IEEE Trans. Antennas Propag.*, vol. 53, no. 9, pp. 2827–2833, Sep. 2005.

[6] F. K. Schwering and S.-T. Peng, "Design of dielectric grating antennas for millimeter-wave applications," *IEEE Trans. Microw. Theory Techn.*, vol. 31, no. 2, pp. 199–209, Feb. 1983.

[7] S.-T. Peng, T. Tamir, and H. L. Bertoni, "Theory of periodic dielect waveguides," *IEEE Trans. Microw. Theory Techn.*, vol. 23, no. 1, pp. 123–133, Jan. 1975.

[8] S. Xu, J. Min, S.-T. Peng, and F. K. Schwering, "A millimeter-wave omnidirectional circular dielectric rod grating antenna," *IEEE Trans. Antennas Propag.*, vol. 39, no. 7, pp. 883–891, Jul. 1991.

[9] S. Xu and X. Wu, "A millimeter-wave omnidirectional dielectric rod metallic grating antenna," *IEEE Trans. Antennas Propag.*, vol. 44, no. 1, pp. 74–79, Jan. 1996.

[10] H. F. Hammad, Y. M. M. Antar, A. P. Freundorfer, and M. Sayer, "A new dielectric grating antenna at millimeter wave frequency," *IEEE Trans. Antennas Propag.*, vol. 52, no. 1, pp. 36–44, Jan. 2004.

[11] L. Huang, J.-C. Chiao, and M. P. D. Lisio, "An electronically switchable leaky wave antenna," *IEEE Trans. Antennas Propag.*, vol. 48, no. 11, pp. 1769–1772, Nov. 2000.

[12] A. Khidre, K. F. Lee, A. Z. Elsherbeni, and F. Yang, "Wide band dual-beam U-slot microstrip antenna," *IEEE Trans. Antennas Propag.*, vol. 61, no. 3, pp. 1415–1418, Mar. 2013.

[13] C.-C. Lin and C.-K. C. Tzuang, "A dual-beam micro-CPW leaky-mode antenna," *IEEE Trans. Antennas Propag.*, vol. 48, no. 2, pp. 310–316, Feb. 2000.

[14] C. Luxey and J.-M. Latheurte, "Simple design of dual-beam leaky-wave antennas in microstrips," *IEE Proc.-Microw., Antennas Propag.*, vol. 144, no. 6, pp. 397–402, Dec. 1997.

[15] Y. Li, Q. Xue, E. K.-N. Yung, and Y. Long, "Dual-beam steering microstrip leaky wave antenna with fixed operating frequency," *IEEE Trans. Antennas Propag.*, vol. 56, no. 1, pp. 248–252, Jan. 2008.

[16] C.-J. Wang, C. F. Jou, and J.-J. Wu, "A novel two-beam scanning active leaky-wave antenna," *IEEE Trans. Antennas Propag.*, vol. 47, no. 8, pp. 1314–1317, Aug. 1999.

[17] C.-J. Wang, "Active dual-beam leaky-wave antenna with asymmetrically scanning capability," *Electron. Lett.*, vol. 37, no. 11, pp. 672–673, May 2001.

[18] T.-L. Chen and Y.-D. Lin, "Dual-beam microstrip leaky-wave array excited by aperture-coupling method," *IEEE Trans. Antennas Propag.*, vol. 51, no. 9, pp. 2496–2498, Sep. 2003.

[19] C.-C. Hu, C. F. Jsu, and J.-J. Wu, "An aperture-coupled linear microstrip leaky-wave antenna array with two-dimensional dual-beam scanning capability," *IEEE Trans. Antennas Propag.*, vol. 48, no. 6, pp. 909–913, Jun. 2000.

[20] Z. L. Ma, L. J. Jiang, S. Gupta, and W. E. I. Sha, "Dispersion characteristics analysis of one dimensional multiple periodic structures and their applications to antennas," *IEEE Trans. Antennas Propag.*, vol. 63, no. 1, pp. 113–121, Jan. 2015.

[21] A. M. Patel and A. Grbic, "A printed leaky-wave antenna based on a sinusoidally-modulated reactance surface," *IEEE Trans. Antennas Propag.*, vol. 59, no. 6, pp. 2087–2096, Jun. 2011.